16th World Conference on Earthquake, 16WCEE 2017
Santiago Chile, January 9th to 13th 2017
Paper N° 4613
Registration Code: S-F1463239810

LOSS ASSESSMENT OF STEEL MRF BUILDINGS WITH PARTIAL-STRENGTH CONNECTIONS

R. Roldán[1], G. Della Corte[2], T. Sullivan[3]

[1] Design Engineer, Englekirk, Los Angeles, ricardo.roldan@englekirk.com
[2] Associate Professor, University of Naples Federico II, gaetano.dellacorte@unina.it
[3] Associate Professor, University of Canterbury at Christchurch, timothy.sullivan@canterbury.ac.nz

Abstract

Performance expectations of modern societies are increasing worldwide and hence, the computation of time-based losses due to seismic events is gaining relevance. Recent and ongoing studies on the performance-based earthquake engineering framework have illustrated concepts and applications of the approach for a wide range of structural configurations and materials. However, little information is available about timed-based losses of steel moment-resisting frames (MRFs) with partial-strength beam-to-column connections. In particular, bolted partial-strength connections are envisaged to have advantages over full-strength connections in zones of low-to-moderate seismic intensity, because of the lower initial cost as well as easier dismantling (or, eventually, demolition) of the whole structure or parts of it. Unfortunately, there is relatively limited knowledge about the seismic response of partial-strength connections, especially in terms of probabilistic characterization of their performance. Consequently, as a first step, a collection of experimental data, from a previous study on partial-strength moment connections made of bolted end-plates, was statistically analysed to derive component fragility curves. As a second step, a case-study steel building with a lateral force resisting system comprising MRFs with partial-strength connections was designed assuming a site of medium seismic intensity in Italy (i.e., the city of Naples). Non-linear response-history analyses were subsequently carried out using a set of purposely selected ground motions. Finally, a time-based loss assessment was conducted, considering both structural and non-structural elements. The total expected annual losses obtained from the loss assessment were seen to be contributed by approximately 30% by structural (i.e., joint) damage, which is a significant contribution although the largest part is still due to non-structural components. The probability of structural collapse was also seen to be particularly small, thus leading to a correspondingly small contribution of replacement costs to the total costs. This is explained to be a consequence of the MRFs having lateral-force resistance largely exceeding the minimum requirements from seismic design actions, because gravity and wind loads dominated the design. Although the numerical results shown in this (simplified) study should not be seen as a precise or general quantification of losses in actual buildings, the study suggests that steel MRF systems with partial strength joints should be investigated further as a potentially cost-effective design option, especially in low-to-moderate seismic intensity zones.

Keywords: Fragility; Loss assessment; Moment-resisting frames; Partial-strength connections.

1. Introduction

Many advancements in the field of performance-based earthquake engineering (PBEE) have recently been made, highlighting the need for the inclusion of probabilistic methods to deal comprehensively with the uncertainties inherent in any structural seismic design or assessment procedure [1]. Additionally, the need to evaluate seismic performance with metrics most useful to decision makers, (i.e., in terms of expected monetary losses, as well as the number of fatalities and probability of collapse) has also been noted to enhance the practical utility of PBEE procedures [2, 3, 4, 5, 6, 7]. The process of estimating earthquake-induced losses for a building is generally broken into four phases: 1) estimating seismic hazard at the building site; 2) assessing seismic demands to the building for different intensity levels; 3) assessing physical damage to the building (including its content) as a function of seismic demands; and 4) converting physical damage into economic losses. The ATC-58 guidelines [6] detail one possible method for implementing in practice the above general phases. Notwithstanding such significant advancements, the quantification of structural performance in terms of expected losses still faces numerous challenges, especially for what regards the implementation of phases 3 and 4 described above.

Within the above context, this article presents some of the on-going research efforts in Italy, within a project sponsored by the ReLUIS Consortium (Italian network of laboratories for research on earthquake engineering) and funded by the Italian Department of Civil Protection (DPC). In particular, this paper provides information about the work done with reference to steel Moment-Resisting Frames (MRFs). Steel MRFs are not frequently used in Italy, perhaps due to the larger construction costs in comparison with reinforced concrete solutions and relatively smaller seismic intensity in comparison with other seismically active regions. Existing steel structures in Italy, especially the older ones, are frequently characterized by the presence of partial-strength moment connections, e.g., bolted end-plate connections. The use of bolted connections for new buildings might also be advantageous, in consideration of the relatively smaller construction as well as dismantling (or, eventually, demolition) costs. In light of this, some research has already been conducted into steel MRFs with partially-restrained moment connections, focussing on the development of a displacement-based seismic design procedure [5, 8]. This work describes recent efforts made to develop fragility curves for partial-strength beam-to-column joints with bolted end-plates. Such component fragility functions represent an essential input data to the seismic loss assessment procedure. Finally, case-study buildings were designed and analysed to evaluate their expected monetary losses by means of the ATC-58 guidelines [6].

2. Fragilities of Partial-Strength Beam-to-Column End-Plate Joints

2.1 Definition of Damage States and Experimental Data

The engineering demand parameter (EDP) used to characterize the occurrence of any damage state in the beam-to-column sub-assemblages is, as usual for these components, the inter-story drift ratio (IDR).

The selected damage states are defined as yielding and failure, which are also termed damage state 1 and 2 (DS1 and DS2) in the following sections. DS1 is defined as the first occurrence of significant yielding in any component of the joint. The yielding drift ratio is consequently defined as the ratio of the (measured) plastic resistance to the (measured) initial stiffness of the beam-to-column joint. DS2 is defined as the state corresponding to the actual resistance falling below the (measured) plastic resistance. In other words, if a beam-to-column joint is in DS2, then its resistance would be smaller than its initial plastic resistance. The occurrence of DS2 was identified by using the envelopes of cyclic-loading test results, thus including eventual strength deterioration due to repetition of plastic deformations.

As shown in Table 1, four sets of experimental data were identified [9]. Data set 1 comprises results for flush end-plate joints where yielding never involves the column web panel zone. Data set 2 includes experimental results relevant to extended end-plate joints, where no yielding was observed to occur in the corresponding column web panel zones. Data set 3 refers again to extended end-plate joints, similar to data set 2, but all the relevant test results available for this type of connection were included in this set (i.e., in some of the specimens of data set 3 yielding might have occurred in the column web panel zone). Finally, data set 4 comprises results

for only the connections (with extended end-plates). Detailed description of the experimental results used for the data set can be found in [9].

2.2 Variables and Parameters for Statistical Simulations

To generate a statistically meaningful sample of beam-column joints, a mixture of the experimental data described previously and randomly generated beam-column joint properties was used. Description of the specific values used for the simulations can be found in [10].

The beam-to-column joint was characterised by the following parameters: inter-storey height, length of beam span, beam section, column section, material properties and connection characteristics. The characteristics of the connections included: plastic rotation capacity (θ_p), ratio of the joint-to-beam plastic moment resistance ($m_{R,j}$), joint rotational stiffness relative to the connected beam flexural stiffness (k_j) as defined by EN 1993-1-8 [11]. Only some of these variables were treated as fully random, while the others were treated as parameters to be varied within pre-selected ranges.

First, beam sections were varied from IPE200 to IPE750x173. Subsequently, column sections were selected, in such a way that capacity design criteria were satisfied (with a moment demand of $1.3M_{R,j}$, where $M_{R,j}$ is the moment capacity of the joint). The beam length was randomly generated for the statistical simulation by using a continuous uniform distribution. The boundaries for the uniform distribution of beam length were 5000 mm and 8000 mm. The ranges of variability of $m_{R,j}$ and k_j were 0.4-1.0 and 15-25 respectively.

The steel yield strength was assigned a log-normal distribution, with a Coefficient of Variation CoV of 0.07 [12]. Finally, the steel Young's modulus, *E*, was assumed to be constant and equal to 210 GPa [11].

2.3 Fragility Functions Formulation

A component fragility function provides the probability of being in a certain damage state conditioned on the value of a single demand parameter (that is the IDR in the case examined here). For the construction of a fragility function relevant to a damage state, first the data were sorted in ascending order by the demand parameter (i.e., IDR) at which the damage state was reported to occur for each specimen. The cumulative frequency distribution of the experimental IDRs was then obtained with the so-called Hazen's model [13], as follows:

$$P = \frac{i - 0.5}{N} \tag{1}$$

where *N* is the number of experimental points and *i* is the position of the demand parameter within the sorted data. An important advantage of Hazen's model is the fact that it avoids the scenario in which the first data point of a sample is assigned a P of 0 (which is unrealistic), and the last data point with a probability of occurrence of 1.

Normal and Log-Normal probability distributions were subsequently examined to fit the experimental cumulative frequency distributions with continuous cumulative distribution functions (CDFs). For any examined distribution, goodness-of-fit tests were also carried out. The Lilliefors' test [14], which is applicable when the parameters of the function to be tested are estimated from the same data as those being compared with the distribution, was adopted. Therefore, the maximum difference between the adopted mathematical model and the actual discrete distributions was computed with Equation 2:

$$D_i = \max_x \left| F_i - S_M \right| \tag{2}$$

where F_i is the assumed theoretical cumulative distribution function, and S_M is the experimental (empirical) cumulative frequency. An important value that can be obtained from Lilliefors's test is the so called *p*-value [15]. The p-value is useful if the hypothesis that the selected CDF does not represent the experimental data is rejected, because it provides the significance level at which the test would fail in rejecting the hypothesis.

2.4 Fragility Functions for Loss Assessment

Table 1 shows the parameters of the fitted CDFs of the IDR, with reference to each experimental data set as described previously. Corresponding *p*-values from the Lilliefors' goodness-of-fit tests are also provided in the table.

In Fig. 1 the fragility curves resulting from the procedure described above, for each of the four data sets, are shown. The figure shows also results of the Lilliefors' goodness-of-fit tests for normality or lognormality. As shown in the Figure, data sets 1 and 4 passed the test for normal distributions, while data sets 2 and 3 passed the test for lognormal distributions for a significance level of 5%.

Table 1 Statistical parameters of IDR in milliradians (mean, standard deviation and *p*-values) for each data set

				Normal distribution		**Log-normal distribution**		**Lilliefors *p*-value**	
	Data set ID		**No. of samples**	**μ**	**σ**	**θ**	**β**	**Normal**	**Lognormal**
DS1: Plastic moment capacity is developed at the joint	1	Flush end-plate joints with no panel zone yielding	16	12.6	4.2	11.4	0.35	0.20	>0.50
	2	Extended end-plate joints with no panel zone yielding	28	9.3	3.5	9.6	0.48	0.16	<0.001(2)
	3	Extended end-plate joints with or without panel zone yielding	40	8.2	3.3	8.2	0.45	0.40	0.15
	3(1)	Extended end-plate joints with or without panel zone yielding	10000(1)	-	-	11.0	0.34	-	-
	4	Extended end-plate connections	25	8.4	3.3	8.3	0.47	0.49	0.01(2)
DS2: Joint resistance falls below its plastic moment capacity	1	Flush end-plate joints with no panel zone yielding	16	40.8	17.2	46.7	0.54	0.13	0.01(2)
	2	Extended end-plate joints with no panel zone yielding	28	40.0	16.9	37.2	0.46	0.01(2)	0.01(2)
	3	Extended end-plate joints with or without panel zone yielding	40	44.3	20.3	37.6	0.47	<0.001(2)	0.11
	3(1)	Extended end-plate joint with or without panel zone yielding	10000(1)	-	-	47.0	0.31	-	-
	4	Extended end-plate connections	25	30.4	15.0	30.8	0.65	0.17	<0.001(2)

(1) From theoretical and Monte Carlo Simulation

(2) Does not pass the Lilliefors test for 5% significance level

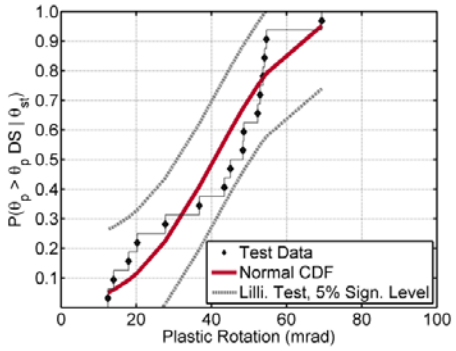

(a.i)

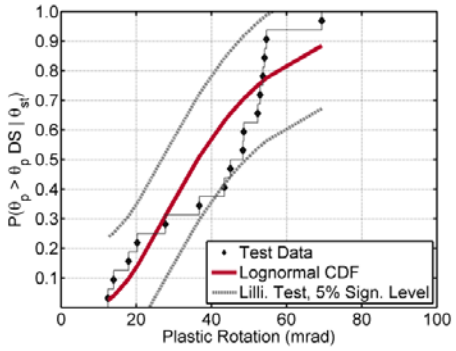

(a.ii)

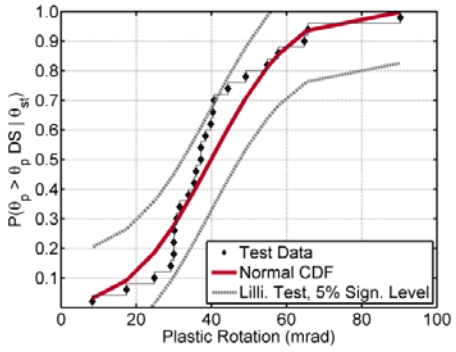

(b.i)

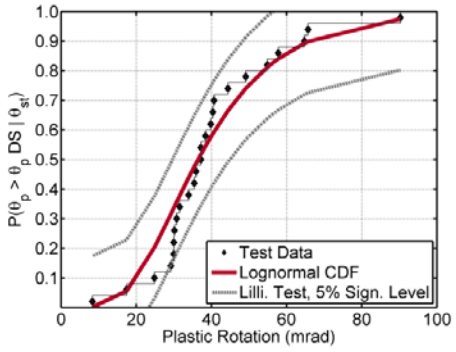

(b.ii)

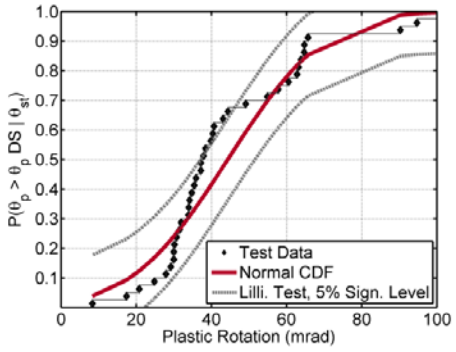

(c.i)

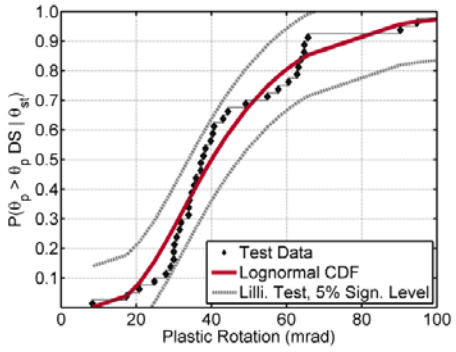

(c.ii)

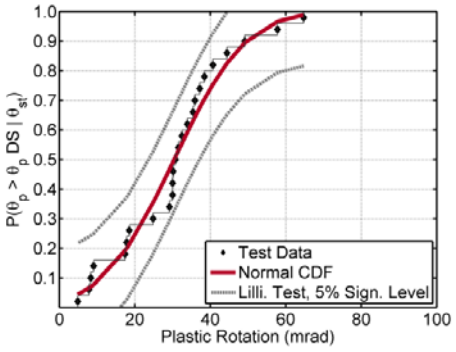

(d.i)

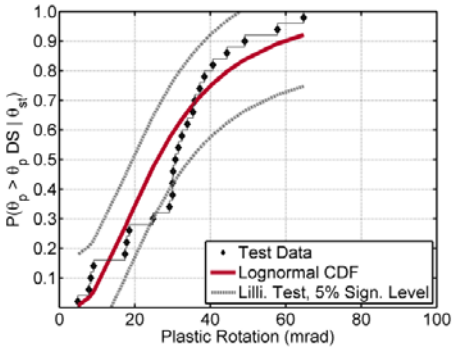

(d.ii)

Fig. 1 Damage state 2: Experimental cumulative frequencies, assumed CDFs and Lilliefors' test results; (a) data set 1, (b) data set 2, (c) data set 3 and (d) data set 4.

3. Case Study Building and Cost Parameters

3.1 General

An 8-storey office building was purposely designed as a case-study. The building was assumed to be located in the city of Naples (Italy), with foundations on a soil profile of rock or rock-like geological formation and including at most 5 m of weaker material at the surface (specified minimum average shear wave velocity in first 30 m of soil, $V_{s,30}$ = 800 m/s, Eurocode 8 soil category A) [16].

The architectural layouts of the lobby and office areas are shown in Fig. 2, where the dry-wall partitions are specified in grey thick lines. Also shown in the figure is the exterior glazing (code B2022.001 from ATC-58). The structural floor layout and frame elevation are shown in Fig. 3. As shown in the figures, moment-resisting steel frames were used in the x- and y-directions, each located at the building perimeter. The building has a constant inter-storey height of 3.5 m, except at the base floor where the inter-storey height is 4.5 m. Along the length (y axis) there are 3 bays of 6.0 m each. Across the width (x axis) the MRF have 3 bays of 6.0 m each. The MRFs in the x axis do not cover the whole length of the building and stop 3 m before each corner.

The gravity load was assumed to consist of a uniformly distributed permanent load G_k = 5.5 kN/m^2 and a uniformly distributed live (imposed) load of Q_k = 3.0 kN/m^2. The live load seismic combination coefficient was assumed equal to 0.3.

Column and beam sections as well as connection parameters are shown in Table 2. The fifth and sixth columns of the table report values of the normalized connection resistance (ratio of strength between connection and beam); the sixth and seventh columns report values of the normalized connection initial stiffness, k_j.

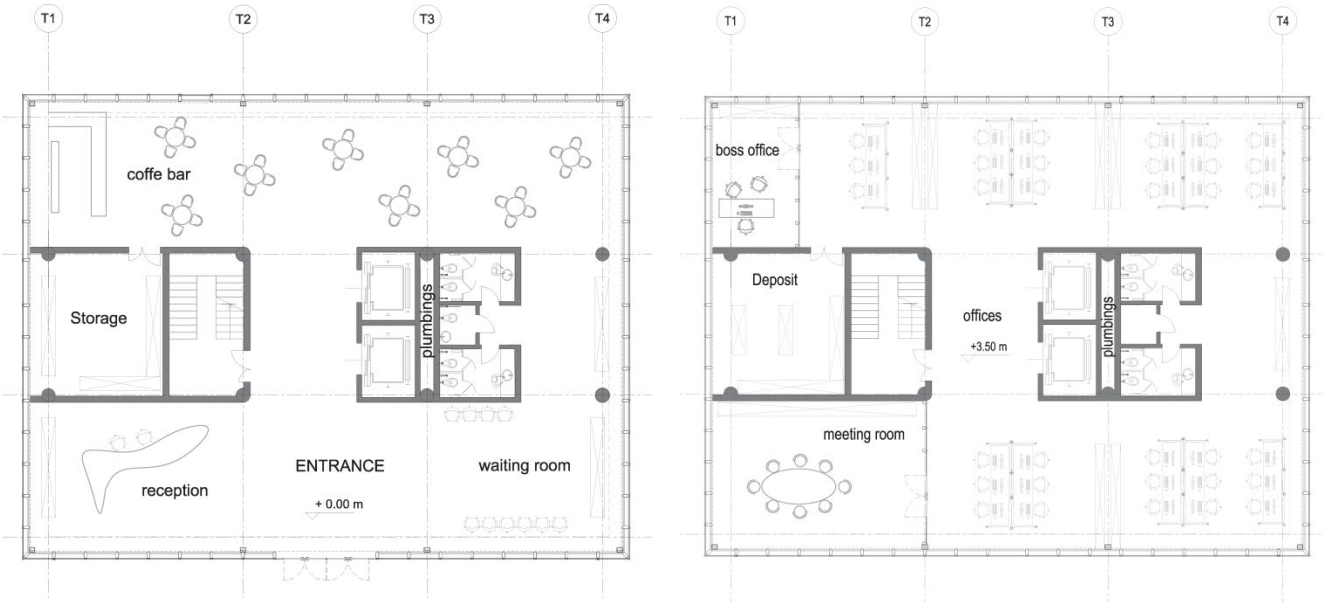

Fig. 2 Architectural layout of the lobby area (left) and architectural layout of the office area (right) for the case study.

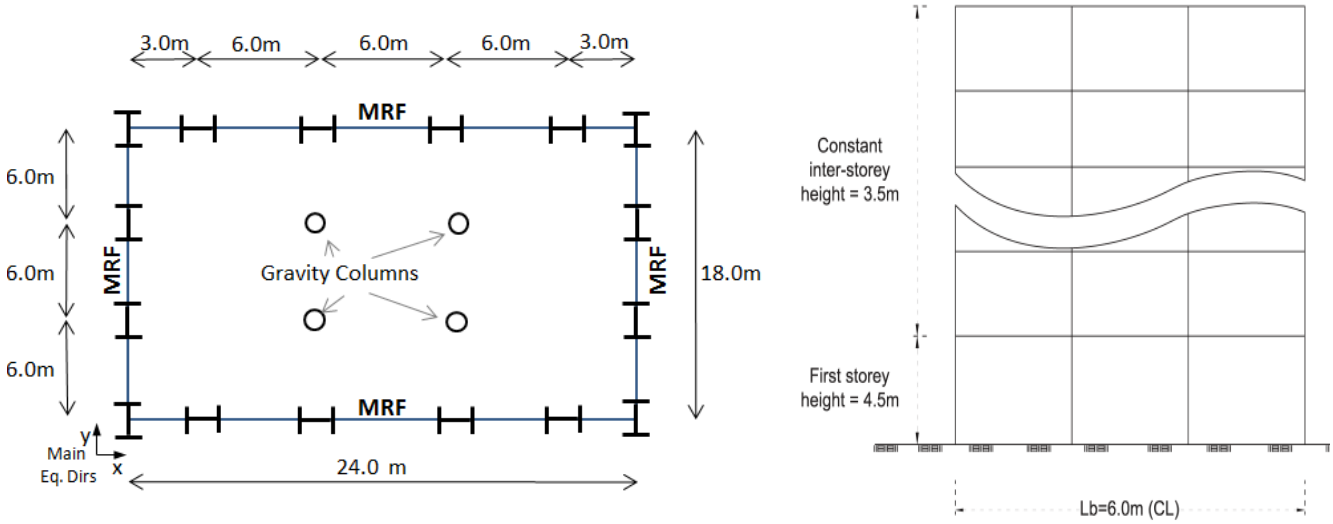

Fig. 3 Structural layout (left) and elevation (right) for the 8-storey case study office building (drawing not to scale).

Table 2 Sections of elements and joint properties.

Storey	Beam Section FINAL-DESIGN	EXT Column Section FINAL-DESIGN	INT Column Section FINAL-DESIGN	$m_{j,EXT-FINAL-DESIGN,i}$	$m_{j,INT-FINAL-DESIGN,i}$	$k_{j,EXT-FINAL-DESIGN,i}$	$k_{j,INT-FINAL-DESIGN,i}$
8	IPE 400	HE 200 A	HE 280 A	0.37	0.56	25	18
7	IPE 400	HE 200 A	HE 280 A	0.37	0.56	25	18
6	IPE 450	HE 200 B	HE 280 B	0.53	0.65	26	25
5	IPE 500	HE 200 B	HE 280 B	0.46	0.56	24	25
4	IPE 500	HE 200 B	HE 280 B	0.46	0.56	24	25
3	IPE 500	HE 200 B	HE 280 M	0.57	0.72	25	29
2	IPE 550	HE 220 M	HE 280 M	0.68	0.60	25	25
1	IPE 550	HE 220 M	HE 280 M	0.68	0.60	25	25

Only the lateral-load resisting system was included as damageable structural components within the probabilistic loss assessment, considering beams, columns and beam-to-column moment connections. Beam and column fragilities were according to information available within PACT (Performance Assessment Calculation Tool) [6], while for the beam-to-column joints the fragility curves illustrated in Fig. 1 were adopted. The quantities of building components were calculated from the case study layouts shown in Fig. 2 and Fig. 3.

To undertake the loss-assessment, the costs of different damage types need to be quantified. The initial construction cost is also needed, as a reference value to which the damage cost is usually related as a percentage. Additionally, in the case of building collapse, the time needed to construct a new building is required, in order to assess indirect damage from downtime of building activities. A summary of the essential figures adopted in this study is provided in Table 3. With reference to this table, the total replacement cost (row 1) was estimated assuming that the core and shell cost (row 4) is 15% of the total cost. Since the unit cost of the structure is estimated as 350 €/m^2, the total replacement cost would be 350/0.15 = 2333.33 €/m^2. With a total floor area of 3456 m^2 (432 m^2 per floor), this calculation leads to a total replacement cost of 2333.33 x 3456 = 8,064,000.00, approximately. The replacement time (row 2) was estimated following the advice of practicing engineers in Italy. In the computation, the demolition process was assumed to last 4 months. The total loss threshold (row 3) is a conventional limit value which was selected as the maximum tolerable economic loss which if exceeded

makes demolition and replacement more reasonable. The maximum number of workers per square meter of the office building plan was again estimated on advice from practicing engineers in Italy.

Table 3 Summary of essential figures for the loss assessment.

Total replacement cost (€):	8,064,000.00
Replacement time (days):	540
Total loss threshold (as ratio of the total replacement cost):	0.4
Core and shell replacement cost (€):	1,209,600.00
Maximum number of workers per square meter:	0.05

3.2 Probabilistic Seismic Hazard Assessment

The probabilistic hazard analysis was conducted for nine hazard levels. The intensity measure (IM) chosen for the case study is the 5% damped spectral acceleration. Hence, the study used ground motion records which were selected and scaled to conditional spectra, created for the site at each intensity level for a conditioning period of 2.0 s [17]. A total number of earthquake events equal to 313 was considered, with moment magnitude (M_w) ranging between 3.0 and 7.9, and epicentre distance up to 337 km. With the selected records, acceleration and displacement mean response spectra for each return period were constructed, as shown in Fig. 4.

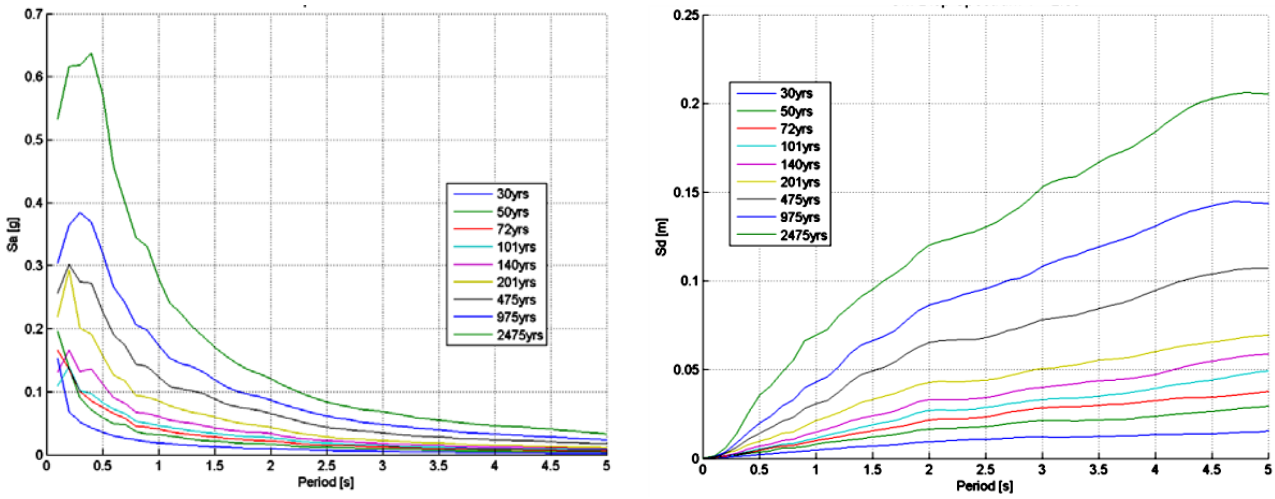

Fig. 4 Mean acceleration spectra (left) and mean displacement spectra (right) of the 30 records for different return periods, conditioned to a period of 2 seconds.

3.3 Structural Analysis

Seismic non-linear time-history analyses (NTHAs) of the case study building were carried out using the software Ruaumoko2D [18]. A two-dimensional frame system with member centre-line dimensions and lumped-plasticity elements was used. Each frame was assigned half of the total seismic mass, assuming rigid floor diaphragm behaviour and disregarding accidental torsional effects.

The analyses were conducted using a Newmark integration scheme. The integration time step was 1/10 of the ground acceleration-history time step, implying integration time steps not greater than 0.0005s. A mass and tangent-stiffness based Rayleigh damping model was used; the elastic damping for the first and second mode was set equal to 3%. Effects on the seismic behaviour from the gravity load applied to the gravity columns identified in Fig. 3 (P-Δ effects), were modelled by lumping gravity loads onto column-elements (known as dummy columns) with pinned ends (assuming that the gravity columns do not provide additional lateral resistance to the system), and using a large displacement analysis option.

Fig. 5 (left) illustrates results from the NTHAs in terms of peak inter-storey drift demand versus spectral acceleration. Results are reported for the nine hazard levels depicted in Fig. 4. Each dot at each intensity level is the response to an individual ground motion. Thick lines correspond to the median of responses, while dashed lines are for the 16th and 84th percentiles. Fig. 5 (right) is similar, but refers to peak floor accelerations (PFAs), which are of interest for evaluating potential damage to the building contents.

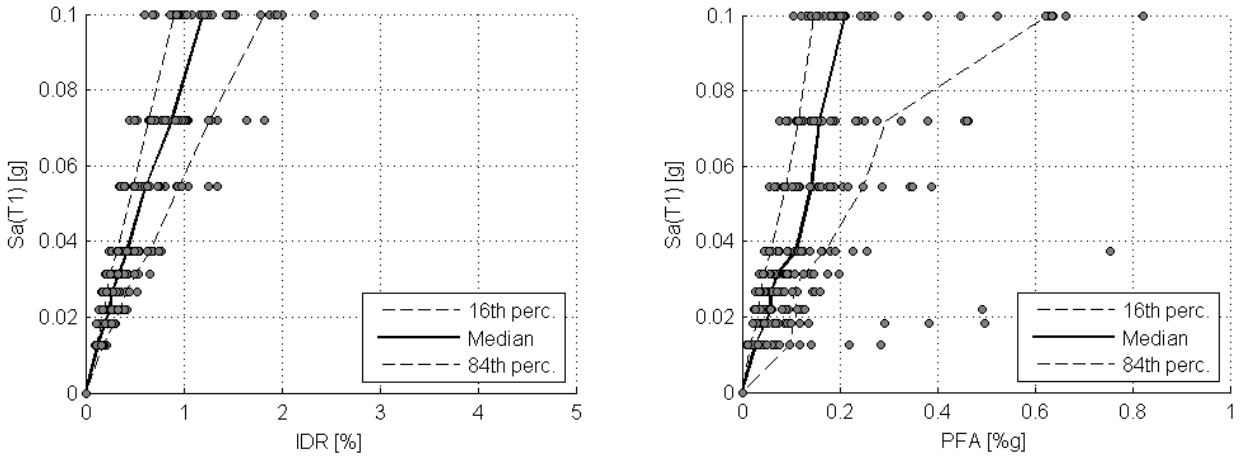

Fig. 5 Incremental dynamic analysis results for inter-storey drift (left) and peak floor acceleration (right).

Using results of the type shown in Fig. 5, fragility curves for different levels of IDRs and PFAs were computed. As an example, Fig. 6 (left) shows the fragility curve obtained for a drift limit of 0.75%. The fragility curve was obtained using standard curve-fitting methodologies.

Given the relatively low seismicity (low design spectral accelerations) at the building site and because of the wind design requirements for serviceability (limitation of displacements), the structure was characterized by resistance largely in excess of the minimum needed to counteract the design seismic actions. Consequently, it exhibited no collapse under any of the ground motions considered, even at the largest spectral acceleration levels (ninth level of hazard). In order to obtain information about the collapse response of the structure, records relevant to an earthquake return period of 2475 years were scaled up to increasing intensities, by multiplying accelerations with the following coefficients: 1.2, 1.5, 2.0, 2.5, 3.0, 3.5, 4.0, 4.5 and 5.0. The corresponding collapse fragility curve is plotted in Fig. 6 (right). The median in terms of $S_a(T^*)$ is 1.91g with a dispersion of 0.72 (where T^* is the specified conditioning period of 2.0s used in this work).

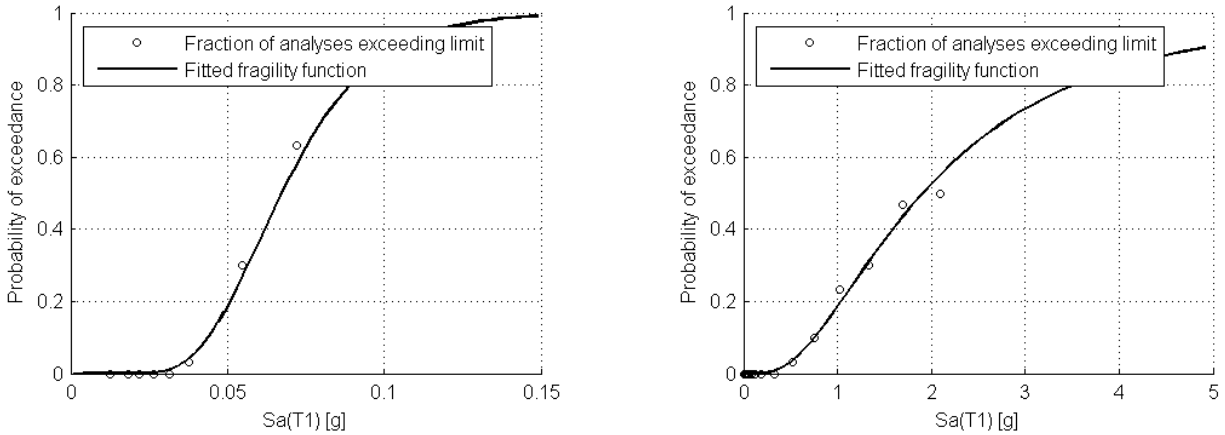

Fig. 6 Fragility curve fitted with the data from NTHA showing the probability of exceeding the drift limit of 0.75% for the DLLS design (left) and the collapse state (right).

4. Loss Estimation

The direct losses are the building repair or replacement costs for earthquake-induced damage. The total repair cost was calculated by summing the mean repair cost over all damageable components in the building and across the nine hazard levels described in section 3.2. The losses computation was not adjusted for inflation or discount rates.

For the computation of direct losses, two different models were built in PACT [6]. One takes into account damage to connections and the associated repair cost, while the other model does not take into account damage to connections. Having these two different results helps to gauge the impact of the connection damage on the loss estimation results. For both PACT models, the information provided in section 3 was utilized. In particular, it is noted that the EDP distributions shown in Fig. 5 were assumed in X and Y directions. (The adopted conversion factor between US Dollars, used in PACT and Euros, used in Table 3, was 1.108 USD for 1 EUR.)

Fig. 7 (top) shows the annual probability that the total repair cost of the building is larger than a certain repair cost value ($C). This is shown for the model without specific consideration of damage in the connections (Fig. 7, top-left) and for the model with specific consideration of damage in the connections (Fig. 7, top-right). Also shown in the figure, is the expected annual loss (EAL) or total annualized repair cost. As expected, the EAL is larger for the model with specific consideration of damage in the connections. The difference between the EALs calculated with and without joint damage is 31% of the EAL including joints; the latter is clearly taken as a more realistic evaluation of costs. Although the inclusion of structural (i.e., joint) damage is significant, the largest part of repair costs is due to the damage to non-structural components.

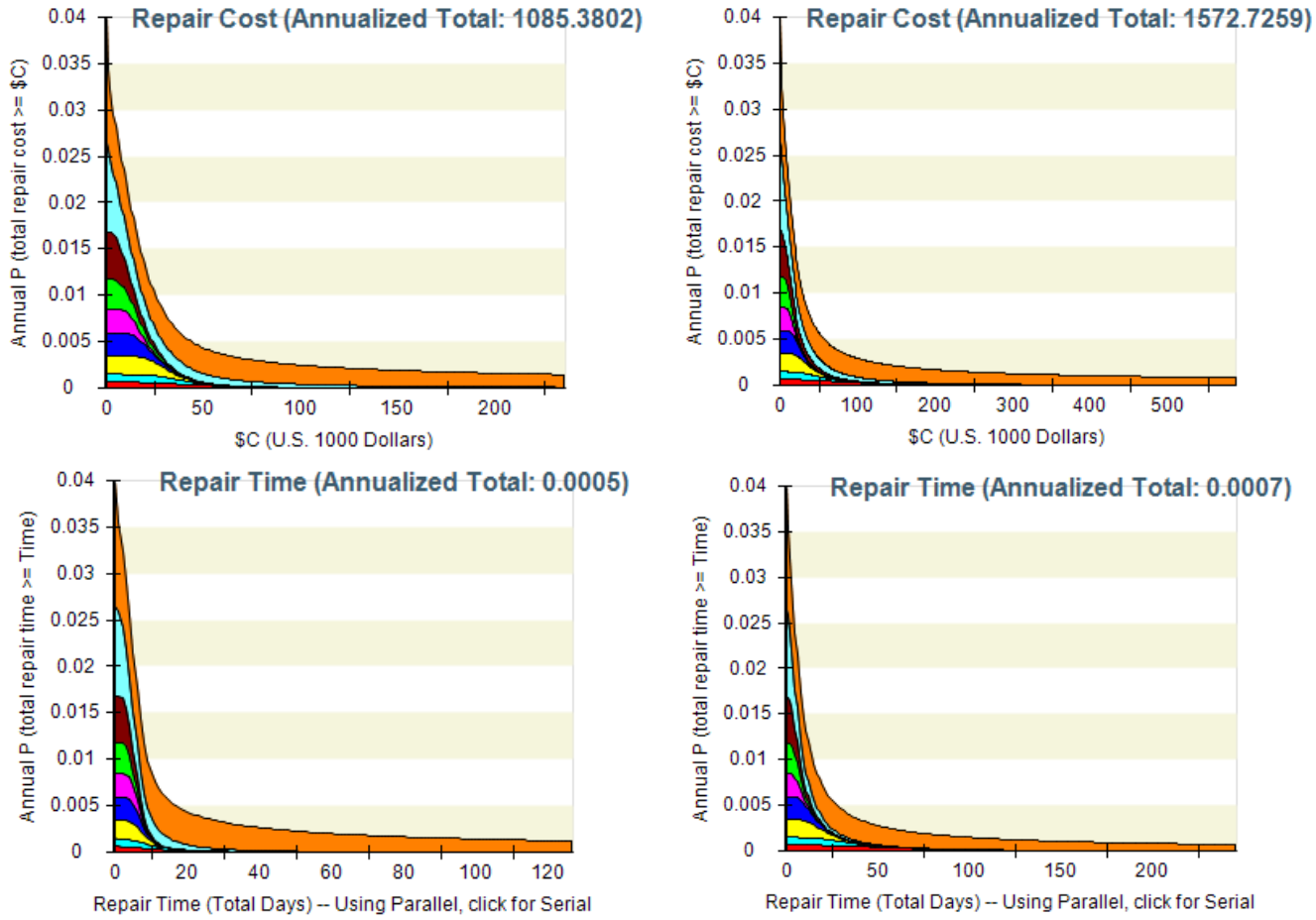

Fig. 7 Time based repair cost model without consideration of connections (top-left) and model with specific consideration of connections (top-right). Time based repair time without consideration of connections (bottom-left) and model with specific consideration of connections (bottom-right).

Fig. 7 (bottom) shows the annual probability of the total repair time of the building being larger than a certain repair time value (total days). This is shown for the model without specific consideration of damage in the connections (Fig. 7, bottom-left) and for the model with specific consideration of damage in the connections (Fig. 7, bottom-right). Also shown in the figure, is the total annualized repair time. As expected, this value is larger for the model with specific consideration of damage in the connections. The difference is 29% (0.0005 against 0.0007) but the annualized repair time is so short that it can be considered to fall within the range of errors of the method.

The annual probability of collapse, the annual probability of unsafe placards and the annual probability of complete loss due to residual drift is almost 0% for both cases. Thus, it could be concluded that the use of partial strength bolted end-plate joints offers a low risk solution considering life safety and downtime. Furthermore, since the expected annual losses were seen to be only slightly affected by the losses due to joint damage, MRF systems with partial strength joints should be investigated further as a potentially cost-effective design option in low-to-moderate seismic intensity zones where load combinations other than seismic governs the design.

5. Conclusions

Fragility functions for steel end-plate bolted beam-to-column joints were developed based on experimental results from 40 specimens and statistical simulation with Monte-Carlo methods. The fragilities can be used to establish the probability of exceeding two damage states as a function of peak inter-storey drift ratio. The first damage state is characterized by the yielding drift, i.e. development of the plastic moment capacity at the beam-column joint; the second damage state is the inelastic drift capacity, defined as the drift making the resistance to fall below the plastic capacity. These fragility curves were implemented in the software PACT [6], and used together with probabilistic seismic loss assessment methods to calculate the expected losses of steel frames with different connection types. The results of the loss assessment conducted here for an 8-storey office building in Naples (Italy) have indicated that the use of partial strength bolted end-plate joints could offer a low risk solution considering life safety and downtime. Indeed, the probability of building collapse was found to be rather small, essentially because the design of the lateral-force resisting system was governed by non-seismic (i.e., gravity and wind loads) design requirements. The contribution from structural joint damage was equal to approximately 30% of the total losses, which appears to be a significant contribution although the largest part of the losses is still due to non-structural components. Although the loss estimates made in this work should not be seen as a precise or general indication of losses for actual buildings, because of both the various simplifications made in the study and the need for more refined hazard estimation at the building site, the study suggests that MRF systems with partial strength joints should be investigated further as a potentially cost-effective design option, especially in areas of low-to-moderate seismic intensity.

6. Acknowledgements

The study presented in this paper was carried out within an on-going research project sponsored by ReLUIS, which is the Italian network of Universities' laboratories for research on earthquake engineering. The financial support to the research project was provided by the Italian Department of Civil Protection. Authors gratefully acknowledge the sponsorship and funding from ReLUIS and DPC.

7. References

[1] Cornell CA, Jalayer F, Hamburger RO, Foutch DA (2002): Probabilistic basis for 2000 SAC Federal Emergency Management Agency Steel Moment Frame Guidelines. *Journal of Structural Engineering*, **128** (4), 526-553.

[2] Porter KA, Kiremidjian AS, LeGrue JS (2001): Assembly-based vulnerability of buildings and its use in performance evaluation. *Earthquake Spectra*, **17** (2), 29-312.

[3] Porter KA (2003): Overview of PEER's Performance-Based Earthquake Engineering Methodology *Proceeding of the Ninth International Conference on Applications of Statistics and Probability in Engineering*, San Francisco, California, USA.

[4] Aslani H, Miranda E. (2005): Probability-based seismic response analysis. *Engineering Structures*, **27** (8), 1151-1163.

[5] Roldán R, Welch D, Nievas C, Sullivan TJ, Correia A, Calvi GM (2014): Guidelines for the Performance-Based seismic Design of Steel MRF Structures. *Research Report EUCENTRE 2014/02*, EUCENTRE Press, Pavia, Italy

[6] ATC (2011): ATC-58 - Guidelines for Seismic Performance Assessment of Buildings: Volume 1 – Methodology. *ATC 58-1*, Applied Technology Council, Redwood City, California, USA.

[7] FEMA (2012): FEMA P-58-1 - Seismic Performance Assessment of Buildings, Volume 1 – Methodology. *Applied Technology Council*, Redwood City, California.

[8] Roldán R, Sullivan TJ, Della Corte G (2016): Displacement-Based Design of Steel Moment Resisting Frames with Partially-Restrained Beam-to-Column Joints. *Bulletin of Earthquake Engineering*, **14** (4), 1017-1046.

[9] Della Corte G, Terracciano G, Di Lorenzo G, Landolfo R (2014): Characterising Bolted End-Plate Beam-Column Joints Using the Component Method. Chapter 5 in Characterising the Seismic Behaviour of Steel Beam-Column Joints for Seismic Design, Edited by T.J. Sullivan and G.J. O'Reilly. *Research Report EUCENTRE 2014/01*, IUSS Press, Pavia, Italy.

[10] Roldan R (2014): Fragility Functions for End-Plate Bolted Beam-to-Column Joints. *Individual Study Report*, ROSE School – IUSS Pavia, Italy.

[11] CEN (2009): EN 1993-1-8. Eurocode 3: Design of steel structures - Part 1-8: Design of joints. *Comité Européen de Normalisation*, Brussels, Belgium.

[12] JCCS (2001): Probabilistic model code Part 3: Resistance variables. *Joint Committee on Structural Safety.* www.jcss.ethz.ch

[13] Hazen A (1914): Storage to be provided in impounding reservoirs for municipal water supply. *Transactions of the American Society of Civil Engineers*, **LXXVII** (Paper 1308), 1539–1659.

[14] Lilliefors H (1967): On the Kolmogorov-Smirnov Test for Normality with Mean and Variance Unknown. *Journal of the American Statistical Association*, **62** (318) 399-402.

[15] Ang A, Tang W (2007): Probability Concepts in Engineering, Emphasis on Applications in Civil and Environmental Engineering. *John Wiley and Sons, Inc.*

[16] CEN (2003): Eurocode 8: Design of structures for earthquake resistance - Part 1: General rules, seismic actions and rules for buildings. *Comité Européen de Normalisation*, Brussels, Belgium.

[17] Ay BO, Fox MJ, Sullivan TJ (2016): Practical challenges facing the selection of spectrum-compatible accelerograms. Technical Note, *Journal of Earthquake Engineering*, in press. DOI: 10.1080/13632469.2016.1157527.

[18] Carr (2008): RUAUMOKO2D – A program for Inelastic Time-History Analysis, Department of Civil Engineering, *University of Canterbury*, Christchurch, New Zealand.